

Dynamic mechanical response of a 1060 Al/Al₂O₃ composite

S. I. HONG*, G. T. GRAY III

Materials Science and Technology Division, Los Alamos National Laboratory, Los Alamos, NM 87545, USA

The flow stress of a 1060 Al/Al₂O₃ composite increases rapidly with strain rate due to the higher dislocation accumulation rate and the increasing strength of dislocation barriers. The Al/Al₂O₃ interfaces were found to be well bonded even after high-rate deformation of the composite. MgAl₂O₄ particles observed at Al/Al₂O₃ interfaces in the composite of the present study are thought to improve the interface strength. Unlike in pure aluminium, a well-developed cell structure was not observed in the deformed 1060 Al/Al₂O₃ composite. The absence of a well-developed cell structure is thought to result from a more homogeneous slip distribution in the composite.

1. Introduction

Recent results reported by Bless *et al.* [1] showing that aluminium-matrix composites were much more efficient at stopping tungsten projectiles than unreinforced aluminium alloys has rendered aluminium-matrix composites more attractive as structural materials under severe loading conditions. Marchand *et al.* [2] and Cho *et al.* [3] have found that for aluminium alloy-matrix composites, dynamic loading raises the value of the critical stress intensity factor for fracture. However, recent work [4] showed more frequent interfacial cracks during dynamic deformation than during quasi-static deformation in an Al–Zn–Mg–Cu alloy–20 vol % SiC composite, which could lower the fracture toughness at high strain rates. Hong *et al.* [4] attributed the more frequent incidence of interfacial cracks at high strain rates to the rapid stress and strain build-up at the interfaces.

In order to develop composites with improved deformation and fracture performance under high loading-rate service environments, it is necessary to understand the microstructural damage and dynamic deformation behaviour of various metal-matrix composites. The correlation between the high-rate stress–strain response and the microstructural evolution in metal-matrix composites has not been examined extensively. The purpose of the present study was to investigate the substructure development and damage at high-strain rates in a commercially pure aluminium-matrix composite reinforced with 10 vol % Al₂O₃. The dislocation structure in a 1060 Al/Al₂O₃ composite after deformation is also compared with that in pure aluminium to investigate the influence of ceramic reinforcement.

2. Experimental procedure

The 1060 Al/Al₂O₃ composite reinforced with

10 vol % α -Al₂O₃ (nominal size 13 μ m) selected for this study was produced by a molten metal method at the Dural Aluminum Composites Corporation at San Diego. This composite was extruded into a rod with a diameter of 25 mm. The as-received composite was heat treated at 450 °C for 12 h and furnace cooled. Compression tests were performed at room temperature with a screw-driven mechanical testing machine at the strain rate of $1 \times 10^{-3} \text{ s}^{-1}$. In order to investigate the strain-rate dependence at high rates, some samples were compressed in a split Hopkinson pressure bar to a total strain of 22% at strain rates between 2×10^3 and $6 \times 10^3 \text{ s}^{-1}$.

Some samples were cut parallel to the extrusion direction before and after deformation for transmission electron microscopy (TEM) characterization. Discs, 3 mm diameter, were mechanically dimpled to 60 μ m centre thickness and ion thinned at 5 kV with an incidence angle between 11° and 12° in a liquid-nitrogen stage. To ensure that the ion-milled samples were first cooled to the lowest temperature the system allows, the ion beams were switched on only after waiting at least 1 h with the specimen rotation drive rod lowered into a dewar containing liquid nitrogen. A detailed description of the preparation of TEM samples is provided elsewhere [5]. TEM observations were carried out using a Phillips CM-30 electron microscope operated at 300 kV. X-ray analysis was conducted with a Kevex X-ray spectrometer fitted with an ultra-thin window for the detection of light elements, including carbon and oxygen.

3. Results

Many small particles were observed to be present near the Al/Al₂O₃ interface regions, as shown in Fig. 1. These particles were identified as spinels and Mg₂Si by X-ray micro-analysis and diffraction analysis [6]. In

*Present address: Department of Metallurgy and Materials Engineering, Kook-Min University, Seoul, Korea.

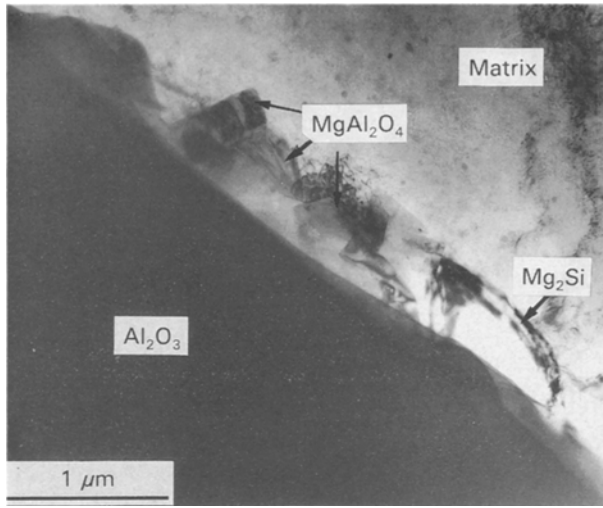


Figure 1 Bright-field transmission electron micrograph of the matrix-interface region in the Al/Al₂O₃ composite.

addition, iron and silicon-rich intermetallic compounds are often observed in the matrix [6]. Fig. 2a and b show the dislocation arrangement near (a) and away from (b) the interface in the composite. Both micrographs were taken using a {111} reflection in a $\langle 110 \rangle$ zone. As shown in these micrographs, the dislocation density is found to be higher near Al/Al₂O₃ interfaces [5]. An interesting finding is that dislocations tend to be distributed more uniformly near Al/Al₂O₃ interfaces (Fig. 2a) while there is some tendency for dislocation clustering in the matrix away from the Al/Al₂O₃ interfaces (Fig. 2b).

Fig. 3 shows the stress-strain response of the composite as a function of strain rate. The stress-strain response of the composite at 77 K and at low strain rate (10^{-3} s^{-1}) is also plotted in this figure and compared with the stress-strain behaviour of the composite deformed at high strain rates, but at room temperature. This figure shows that the strain-rate sensitivity of the 1060 Al/Al₂O₃ composite is small at low strain rates. However, the flow stress is observed to increase quite rapidly at strain rates higher than 1000 s^{-1} . This rapid increase of the flow stress at high strain rates can be readily understood if one compares the high-rate stress-strain response at room temperature with that obtained at low strain rate, but at 77 K.

In Fig. 4a and b, dislocation structures away from interfaces in the composite deformed at room temperature at low ($\dot{\epsilon} = 10^{-3} \text{ s}^{-1}$) and high ($\dot{\epsilon} = 2 \times 10^3 \text{ s}^{-1}$) strain rate are shown, respectively. Dislocations are seen to be arranged in dislocation tangles or loosely knit cell walls at low strain rate at room temperature (Fig. 4a). Following high-rate deformation, dislocations are more randomly distributed although there is some loosely knit cell-wall formation (Fig. 4b).

Fig. 5a and b show dislocation structures near (a) and away from (b) Al/Al₂O₃ interfaces at a higher magnification in the composite deformed at room temperature and at a low strain rate ($\dot{\epsilon} = 10^{-3} \text{ s}^{-1}$). Fig. 6a and b show dislocation structures near (a) and away from (b) Al/Al₂O₃ interfaces at a higher magni-

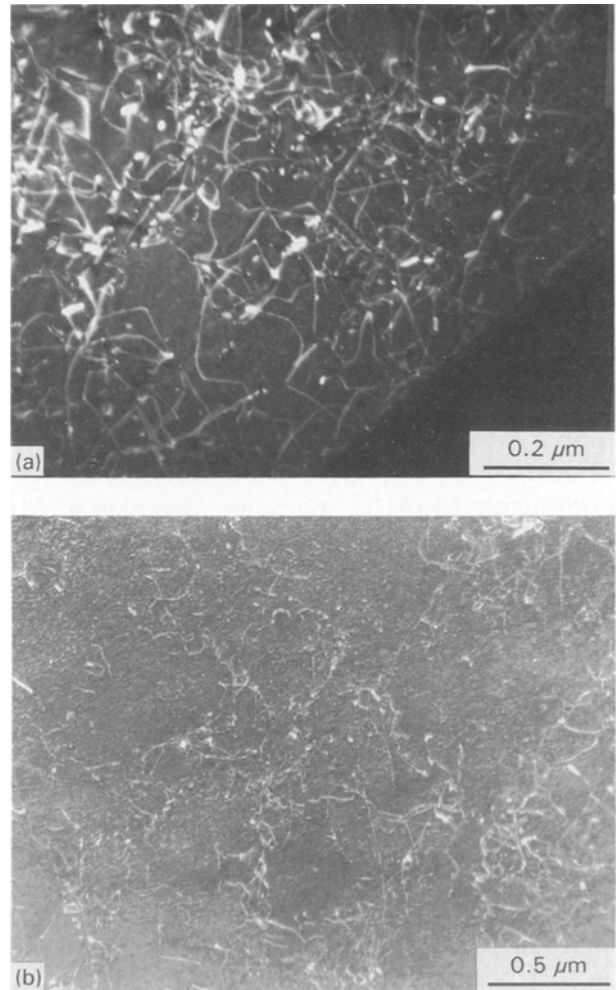


Figure 2 Dark-field transmission electron micrographs of the undeformed Al/Al₂O₃ composite, (a) near the interface, (b) away from the interface.

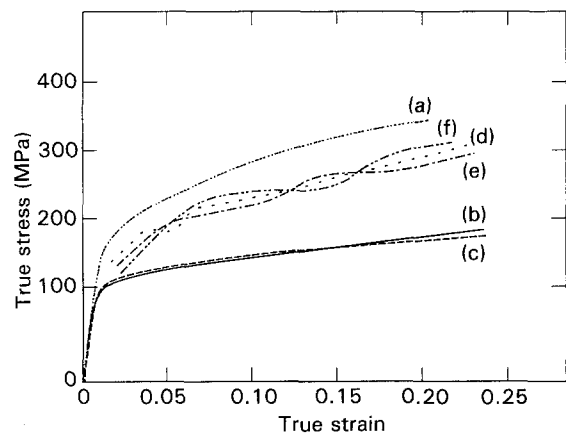


Figure 3 Stress-strain response of the slowly cooled Al/Al₂O₃ composite as a function of strain rate at (a) 77 K and (b-f) 298 K. (a, b) 0.001 s^{-1} , (c) 0.1 s^{-1} , (d) 2000 s^{-1} , (e) 4000 s^{-1} , (f) 6000 s^{-1} .

fication in the composite deformed at room temperature, but at high strain rate ($\dot{\epsilon} = 2 \times 10^3 \text{ s}^{-1}$). In general, the dislocation density is higher following high-rate deformation (compare Figs 4 and 5). At high strain rate and room temperature, however, dislocations are randomly distributed and contain few loosely knit dislocation tangles (Figs 4b and 6). At low strain rate and room temperature, dislocations are

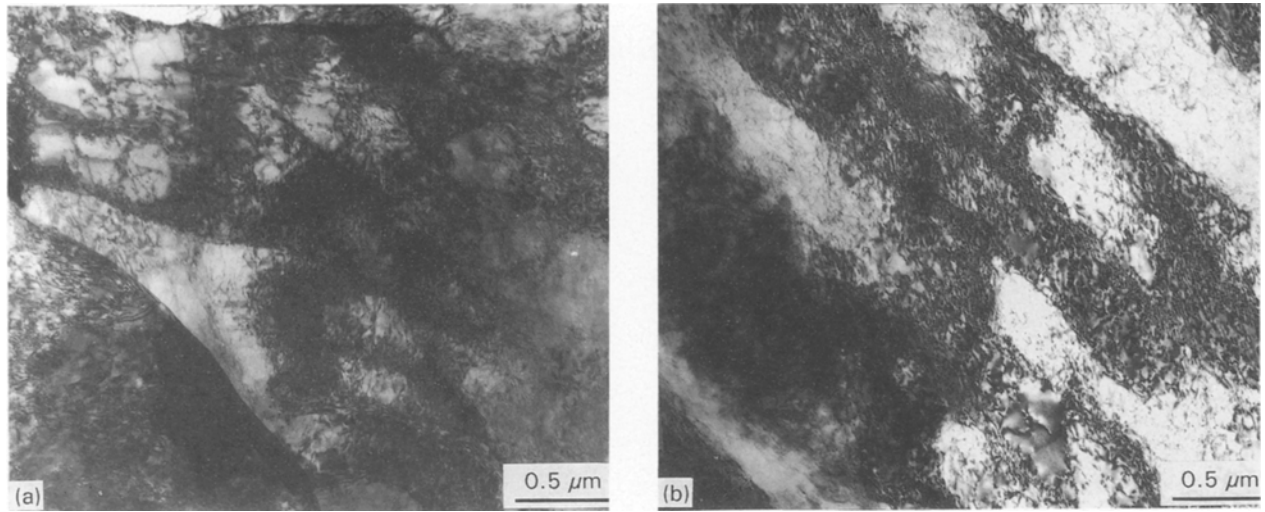


Figure 4 Dislocation arrangement of slowly cooled Al/Al₂O₃ composite deformed at 298 K to $\epsilon = 0.23$, (a) $\dot{\epsilon} = 10^{-3} \text{ s}^{-1}$, (b) $\dot{\epsilon} = 2000 \text{ s}^{-1}$.

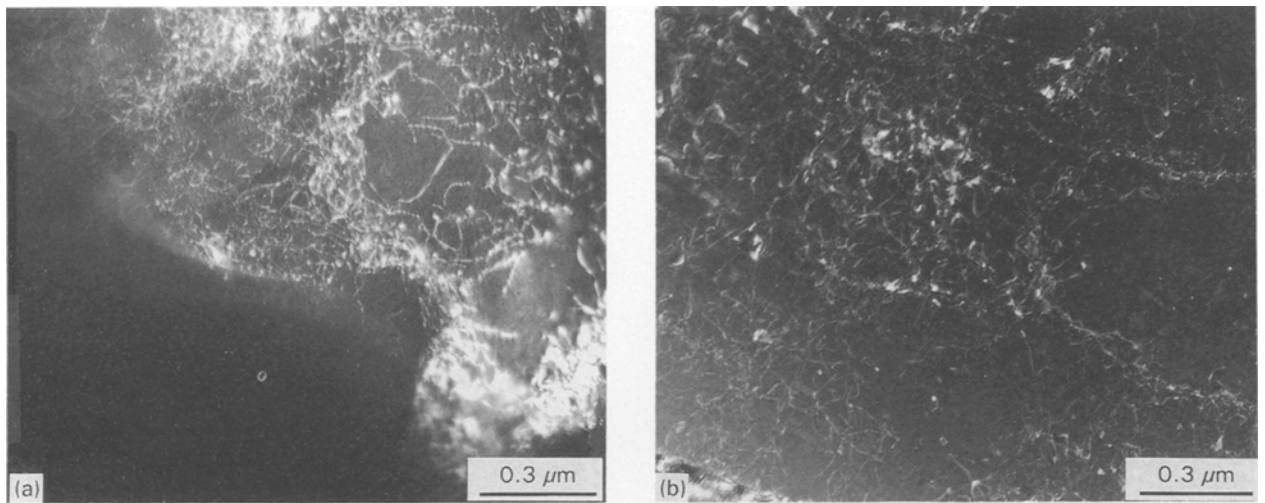


Figure 5 Dark-field transmission electron micrograph of slowly cooled Al/Al₂O₃ composite deformed at a strain rate of 10^{-3} s^{-1} at 298 K to $\epsilon = 0.23$, (a) near the interface region, (b) away from the interface.

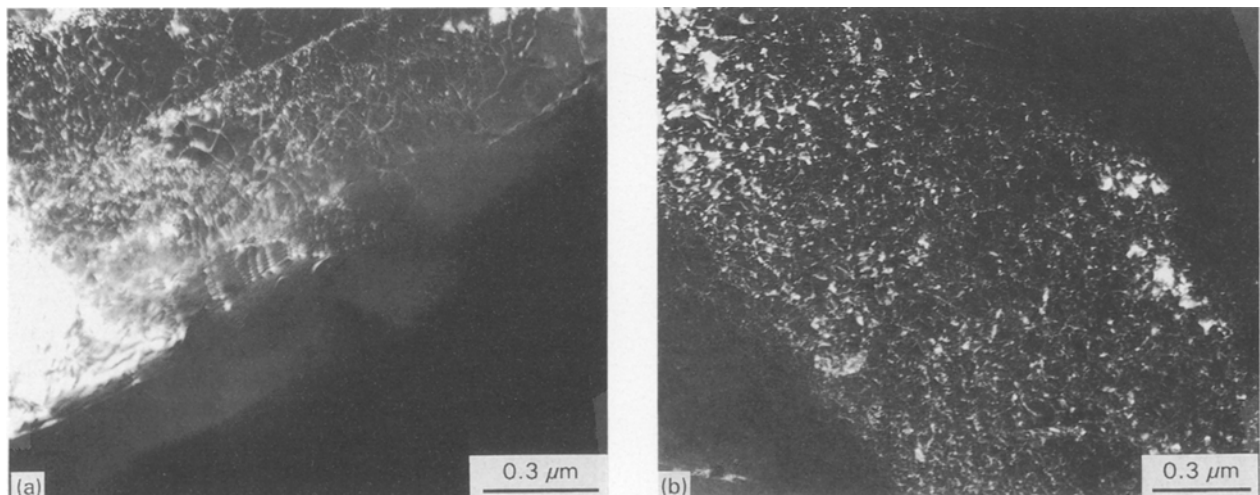


Figure 6 Dark-field transmission electron micrograph of slowly cooled Al/Al₂O₃ composite deformed at the strain rate of 2000 s^{-1} at 298 K to $\epsilon = 0.23$, (a) near interface region, (b) away from the interface.

more tangled and many more loosely knit dislocation cell walls are seen (Figs 4a and 5). This indicates that dislocation rearrangement and recovery are more difficult at high strain rate.

Fig. 7a and b show dislocation structures in the composite deformed at 77 K and at a low strain rate ($\dot{\epsilon} = 10^{-3} \text{ s}^{-1}$). Dislocations are also distributed relatively randomly in the composite deformed at 77 K

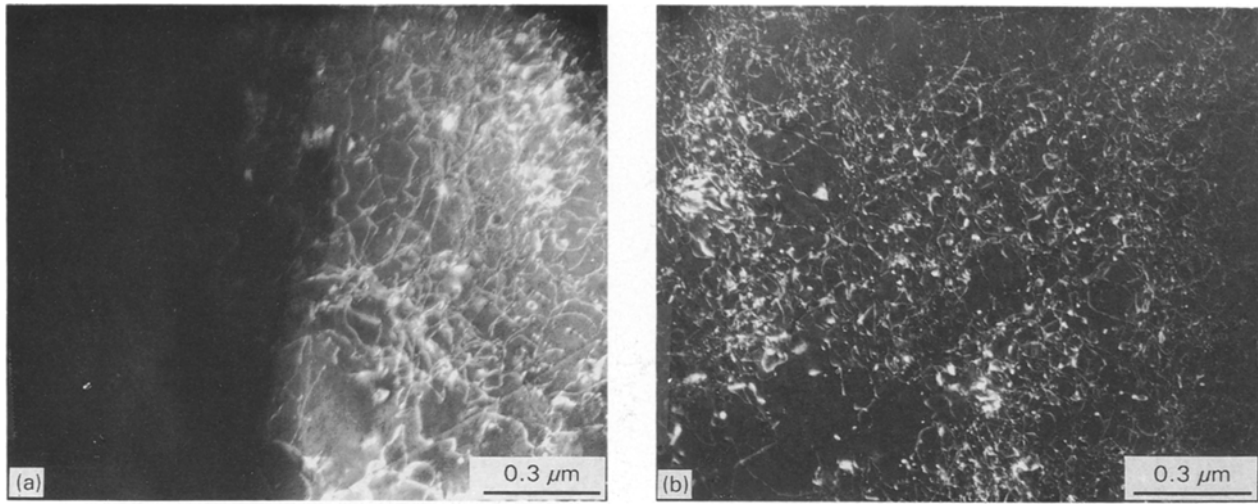


Figure 7 Dark-field transmission electron micrograph of slowly cooled Al/Al₂O₃ composite deformed at a strain rate of 10⁻³ s⁻¹ at 77 K to $\epsilon = 0.23$, (a) near interface region, (b) away from the interface.

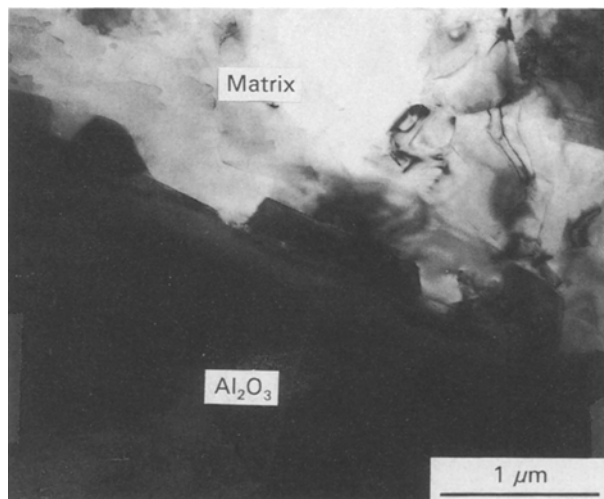


Figure 8 Al/Al₂O₃ interface in slowly cooled composite deformed at the strain rate of 2000 s⁻¹ at 298 K to $\epsilon = 0.23$.

and at a low strain rate ($\dot{\epsilon} = 10^{-3}$ s⁻¹). As shown in Figs 5–7, dislocations are more homogeneously distributed near Al/Al₂O₃ interfaces even after the composite is deformed to a total strain of 0.23. It can be noted that the interfaces in the 1060 Al/Al₂O₃ composite are well bonded even after high strain-rate deformation as shown in Fig. 8, consistent with the rapid increase of the flow stress at high strain rates. The presence of spinels at Al/Al₂O₃ interfaces are known to increase the interface strength in Al/Al₂O₃ composites [7].

4. Discussion

The rapid increase of the flow stress at high strain rates or low temperature can be explained by the rapid accumulation of dislocations and increasing resistance to dislocation motion. Because there are no other appreciable thermal barriers in a slowly cooled commercially pure aluminium-matrix composite, dislocation intersectioning could be the rate-controlling

mechanism in the present composite, as observed for pure aluminium [8, 9]. The rapid increase of the flow stresses observed in the 1060 Al/Al₂O₃ composite is in sharp contrast to the observations in Al–Zn–Mg–Cu alloy-matrix composites reinforced with 20 vol % SiC. In this case, the flow stress was found to fall off at high strain rates when the total strain exceeded 15%. The fall in the flow stress was suggested to result from microstructural damage in the Al–Zn–Mg–Cu alloy matrix composites where frequent Al/SiC interfacial cracks are observed [5].

The increase or decrease of the hardening rate in metal-matrix composites as a function of strain rate can be described by the following equation

$$\Theta = \eta[\Theta_h - \Theta_r(\sigma, T, \epsilon) - \Theta_{ad}] \quad (1)$$

where Θ is the total hardening rate, Θ_h is the hardening component due to dislocation generation and storage, Θ_r is the dynamic recovery term due to dislocation rearrangement and storage, and Θ_{ad} is the accumulative damage term due to interface damage or particle cracking at a given temperature and strain rate. Finally, η is the ratio of the strength at two different temperatures or strain rates for the same microstructure. Equation 1 was modified from that used previously [6] to describe the hardening rate in more complex materials such as composites. For example, the Θ_{ad} term is included in Equation 1 because microstructural damage at interfaces or particles can lower the overall hardening rate in a composite. We believe inclusion of the η term in Equation 1 is relevant because the ratio of the flow stresses at two different temperatures or strain rates should be constant, irrespective of total strain, if the Cottrell–Stokes law is obeyed. To keep the ratio of the flow stresses at two different strains constant, the hardening rate should increase. Accordingly, the ratio of hardening rates, η , at two different temperatures or strain rates should be the same as the ratio of flow stresses, if the Cottrell–Stokes law is followed. If the Cottrell–Stokes law is not observed, η at a given strain should be used.

The fall in the flow stresses at high strain rates observed in the Al–Zn–Mg–Cu alloy-matrix composite [4] is suggested to result from an increasing Θ_{ad} term with strain at high strain rates. The rapid increase of flow stresses at high strain rates in the 1060 Al/Al₂O₃ composite suggests that the Θ_{ad} term due to interface or particle cracking is negligible. This is supported in the present study by the observations that the interfaces in our composite were well bonded even after high-rate deformation. At high strain rates the dynamic recovery term, Θ_r , becomes very small because dislocation rearrangement and recovery becomes very difficult, leading to increasing hardening rates.

The frequent interfacial cracks at high rates (for total strains larger than 0.15) in the Al–Zn–Mg–Cu alloy matrix composites are believed to be enhanced by the presence of MgO particles at the interfaces [4, 5]. Conversely, MgAl₂O₄ particles were present at Al/Al₂O₃ interfaces in the present study. It is well known that the interfacial bonding between aluminium and Al₂O₃ particles improves in the presence of MgAl₂O₄ [10].

Unlike pure aluminium, a well-developed cell structure was not observed in the 1060 Al/Al₂O₃ composite even after deformation to a total strain of 20% at room temperature [11]. The typical dislocation structure in pure aluminium deformed to a total strain of 10% is known to consist of a well-developed cell structure [8, 11]. The absence of a well-developed cell structure is thought to result from a more homogeneous slip distribution in the composite. It is well known that the presence of non-shearable precipitates promotes slip homogenization and a more random dislocation substructure [4, 8]. Likewise, the ceramic particles in the composite in the present study are expected to block and thereby diffuse localized slip.

The formation of a well-developed cell structure may be further inhibited by impurities in the composite, although their effect should be minimal given the solubilities of these impurities at room temperature are small [5]. The internal or residual stresses developed in the composite by the thermal expansion mismatch would also favour a relatively random distribution of dislocations. Dislocations punched out from the Al/Al₂O₃ interface due to the thermal expansion coefficient mismatch would tend to be distributed rather randomly to screen the internal stresses [6]. However, because the number and the volume fraction of Al₂O₃ particles are not large, there is still some tendency for the formation of tangles and loosely knit cells in the composite matrix away from Al/Al₂O₃ interfaces.

The observation of a random distribution of dislocations at high strain rates or low temperatures is in sharp contrast to those in pure copper or aluminium deformed at high rates [11, 12]. Dislocation cells were usually observed in pure copper and aluminium deformed at high rates [13, 14]. The more random distribution of dislocations at high strain rates or low temperatures indicates that dislocation rearrangement and recovery is difficult in the composite at high strain rates. The higher flow stress at 77 K and a low strain

rate ($\dot{\epsilon} = 10^{-3} \text{ s}^{-1}$) than that at room temperature and a high strain rate (see Fig. 3) suggests that the thermally activated rearrangement and the recovery of dislocations are more difficult at 77 K.

In this study, quantitative measurements of the macroscopic dislocation density were not made owing to the gradient in the dislocation density adjacent to Al₂O₃ particles and the influence of the Al₂O₃ particle spacing on the local dislocation density. However, TEM observations consistently showed that although the dislocation density increases throughout the matrix after deformation, the increase of the dislocation density is much more pronounced in the matrix away from the Al/Al₂O₃ interfaces than in the near interface regions (see Figs 2, 5–7). This observation seems reasonable, because most of the applied strain would be accommodated primarily by deformation of the soft matrix region away from the more heavily dislocated interfacial regions. This further explains why the strain hardening and deformation behaviour is primarily controlled by the matrix microstructure. Consistent with this, Hong *et al.* [4] recently observed that the hardening behaviour of underaged and overaged Al–Zn–Mg–Cu alloy-matrix composites was not significantly changed by the ceramic reinforcement.

5. Conclusions

On the basis of the present investigation of the dynamic deformation behaviour of a commercially pure aluminium-matrix composite, the following conclusions can be drawn.

1. The rapid increase of the flow stress at high strain rates in 1060 Al/Al₂O₃ composites suggests that microstructural damage in the interface or particle cracking is negligible in compression at high strain rates.
2. The higher dislocation accumulation rate combined with the increasing strength of dislocation barriers increases hardening rates at high strain rates or low temperatures.
3. The interfaces are well bonded even after high-rate deformation in the composites of the present study. MgAl₂O₄ particles observed at the Al/Al₂O₃ interfaces in the composites are thought to improve the interface strength.
4. Unlike in pure aluminium, well-developed cell structures were not observed in the deformed 1060 Al/Al₂O₃ composites. The absence of the well-developed cell structure is thought to result from a more homogeneous slip distribution in the composite deformed in compression.
5. A more random distribution of dislocations at high strain rates or low temperatures indicates that dislocation rearrangement and recovery are difficult during these loading conditions.

Acknowledgements

The authors thank Mike Lopez, Walter Wright and Carl Truhjillo for their excellent support of the experimental portions of this program, and also A. Zurek for reviewing this manuscript. This work was performed

under the auspices of the United States Department of Energy.

References

1. S. J. BLESS, D. L. JURICK and S. P. TIMOTHY, in "International Conference on High Strain Rate Phenomena in Materials", edited by M. A. Meyers, L. E. Murr and K. P. Staudhammer 12-18 August, San Diego (1990).
2. A. MARCHAND, J. DUFFY, T. A. CHRISTMAN and S. SURESH, *Eng. Fract. Mech.* **30** (1988) 295.
3. K. CHO, S. LEE, Y. W. CHANG and J. DUFFY, *Metall. Trans.* **22A** (1991) 367.
4. S. I. HONG, G. T. GRAY III and J. J. LEWANDOWSKI, *Acta Metall. Mater.* **41** (1993) 2337.
5. S. I. HONG and G. T. GRAY III, *Acta Metall. Mater.* **40**, (1992) 3299.
6. S. I. HONG, G. T. GRAY III and K. S. VECCHIO, *Mater. Sci. Eng.* (1994) in press.
7. H. RIBES, M. SUERY, G. L'ESPERANCE and J. G. LEGOUX, *Metall. Trans.* **21A** (1990) 2489.
8. A. K. MUKHERJEE, J. D. MOTE and J. E. DORN, *Trans. AIME* **233** (1965) 1559.
9. D. L. HOLT, S. G. BABCOCK, S. J. GREEN and C. J. MAIDEN, *Trans. ASM* **60** (1967) 152.
10. H. MECKING and U. F. KOCKS, *Acta Metall.* **29** (1981) 1865.
11. P. R. SWANN, in "Electron Microscopy and Strength of Crystals", edited by G. Thomas and J. Washburn (Interscience, New York, 1963) p. 131.
12. J. D. EMBURY, *Metall. Trans.* **16A** (1985) 2191.
13. G. T. GRAY III, P. S. FOLLANSBEE and C. E. FRANTZ, *Mater. Sci. Eng.* **A111** (1989) 9.
14. G. T. GRAY III and J. C. HUANG, *ibid.* **A145** (1991) 21.

*Received 10 March
and accepted 30 November 1993*